Supporting Information

Influence of support texture and reaction conditions on the accumulation and activity in the gas-phase aldol condensation of *n*-pentanal on porous silica

Markus Schörner [1], Stefanie Kämmerle [1], Dorothea Wisser [2], Benjamin Baier [1], Martin Hartmann [2], Matthias Thommes [3], Robert Franke [4,5], Marco Haumann [1]*

1 Friedrich-Alexander-Universität Erlangen-Nürnberg (FAU), Lehrstuhl für Chemische Reaktionstechnik (CRT), Egerlandstr. 3, 91058 Erlangen, Germany

2 Erlangen Center for Interface Research and Catalysis (ECRC), Egerlandstr. 3, 91058 Erlangen, Germany

3 Friedrich-Alexander-Universität Erlangen-Nürnberg (FAU), Lehrstuhl für Thermische Verfahrenstechnik (TVT), Egerlandstr. 3, 91058 Erlangen, Germany

4 Evonik Operations GmbH, Paul-Baumann-Str. 1, D-45772 Marl, Germany

5 Ruhr-Universität Bochum, Lehrstuhl für Theoretische Chemie, Universitätsstr. 150, D-44780 Bochum, Germany

* Corresponding author: marco.haumann@fau.de

23 pages

27 figures

7 tables

Hydrothermal treatment of silica

For hydrothermal treatment of silica, a metal autoclave equipped with a manual pressure indicator, a digital temperature indicator and a pressure release valve was used. The total reactor volume was 300 ml and the autoclave was filled with 16 ml of deionized water at room temperature.

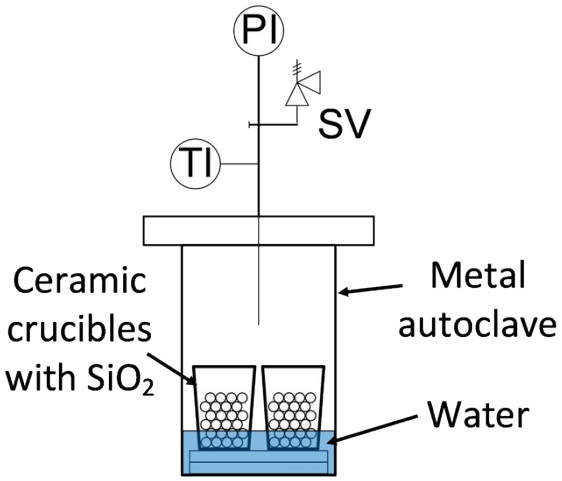

Figure 1. Schematic drawing of autoclave for hydrothermal treatment equipped with pressure indicator (PI), temperature indicator (TI), and pressure release valve (SV).

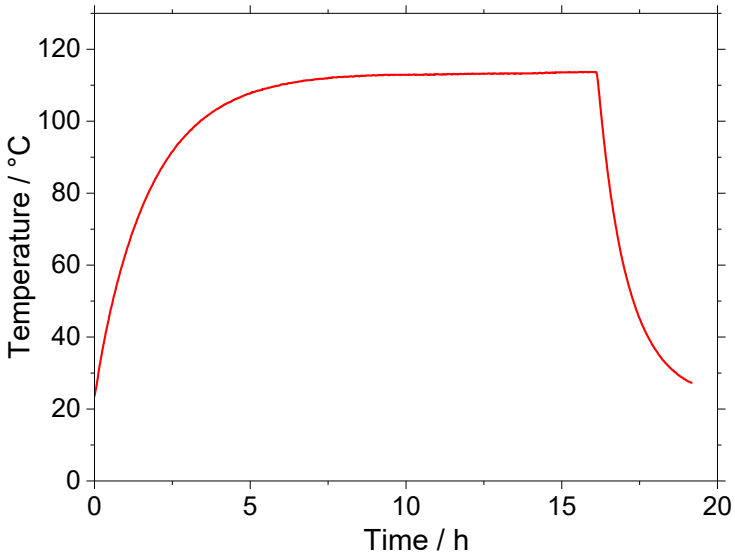

Figure S2. Measured temperature inside the metal autoclave during hydrothermal treatment of silica at 120 °C for 16 h. The autoclave was placed in a preheated oven at t = 0 h and taken out to cool down at t = 16 h.

Gas-phase reactor setup

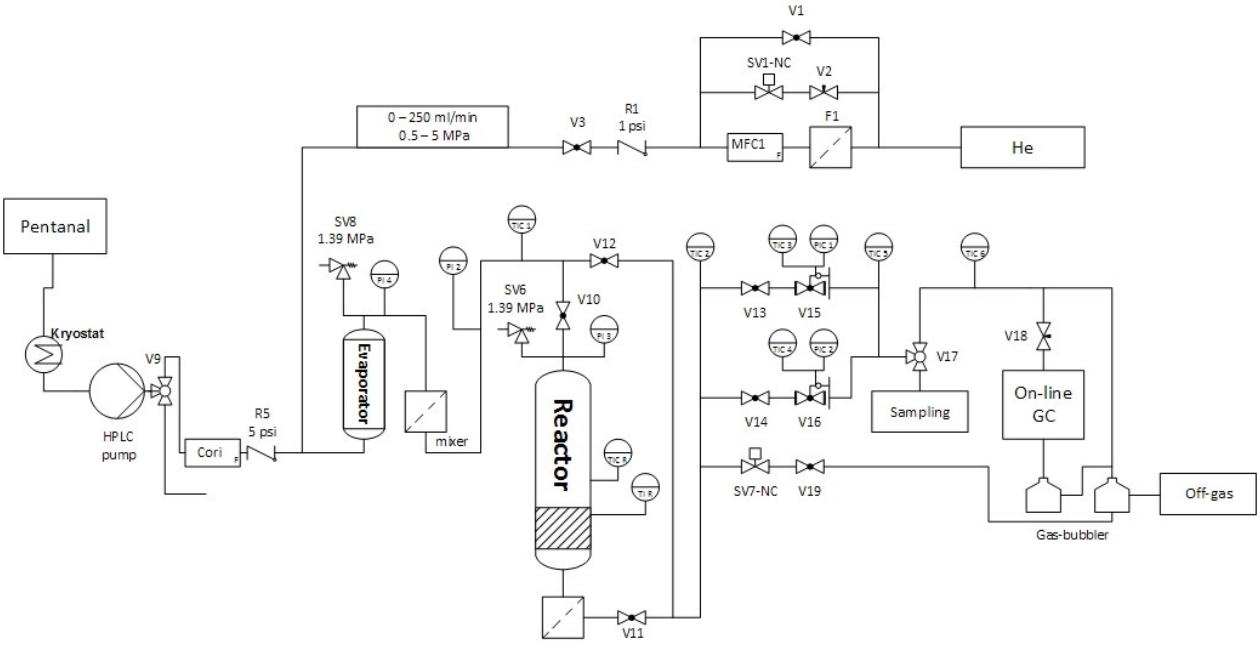

Figure S3. Flow chart of experimental plant.

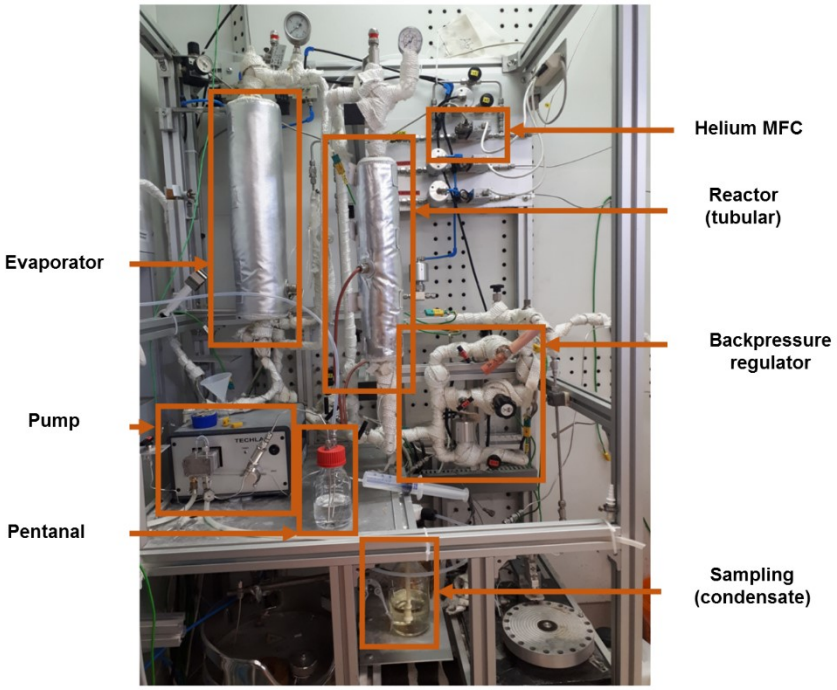

Figure S4. Picture of the gas-phase setup with main parts highlighted.

Texture analysis

N_2-sorption isotherms

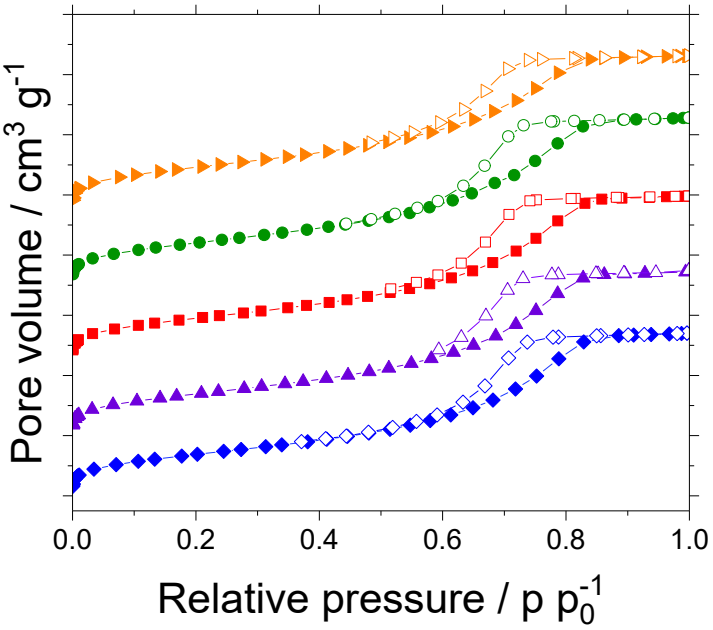

Figure S5. Measured adsorption (filled symbols) and desorption (open symbols) isotherms for untreated silica fractions: 63 – 200 µm (), 200 – 450 µm (), 450 – 630 µm (), 630 – 800 µm (), 800 – 1000 µm ().

Mercury intrusion porosimetry measurement

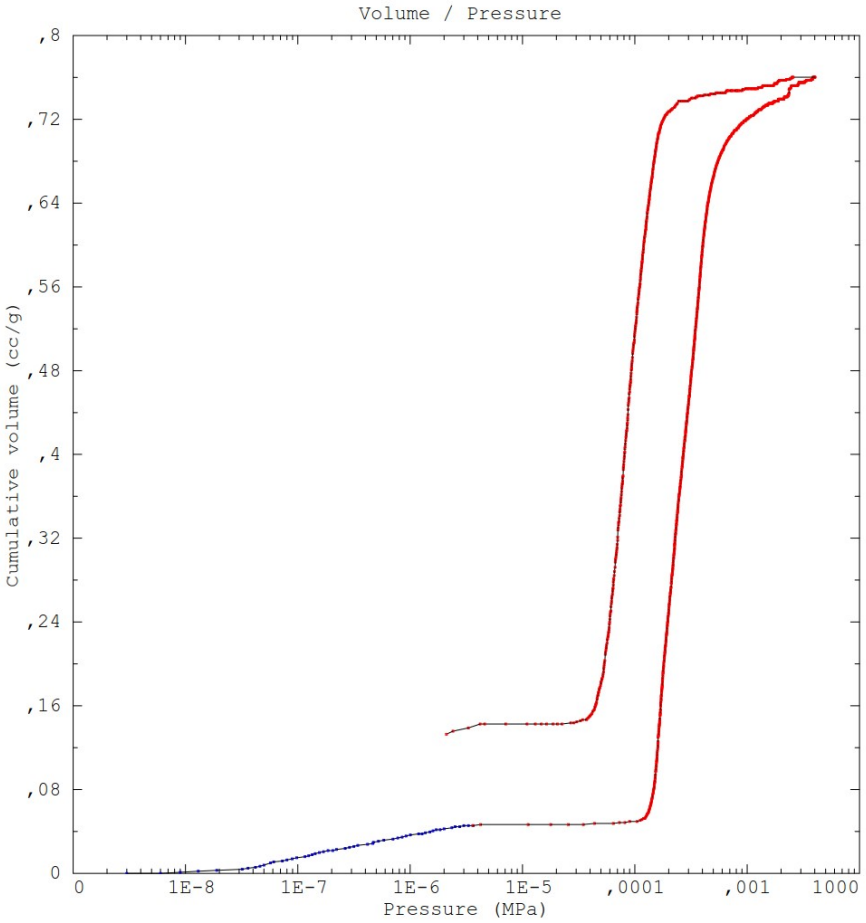

Figure S6. Mercury intrusion porosimetry measurement of silica support, 63 – 200 µm fraction, hydrothermally treated at 180 °C for 24 hours.

Cumulative pore volumes

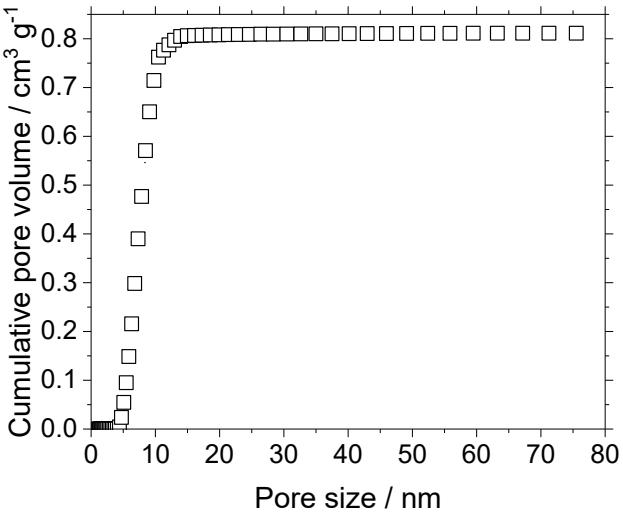

Figure S7. Resulting cumulative pore volume obtained from NLDFT-calculations (adsorption branch) for silica fraction 63 – 200 µm, untreated.

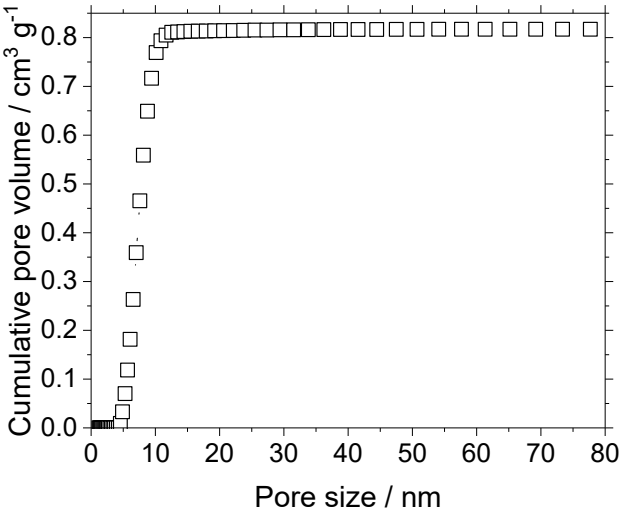

Figure S8. Resulting cumulative pore volume obtained from NLDFT-calculations (adsorption branch) for silica fraction 200 – 450 µm, untreated.

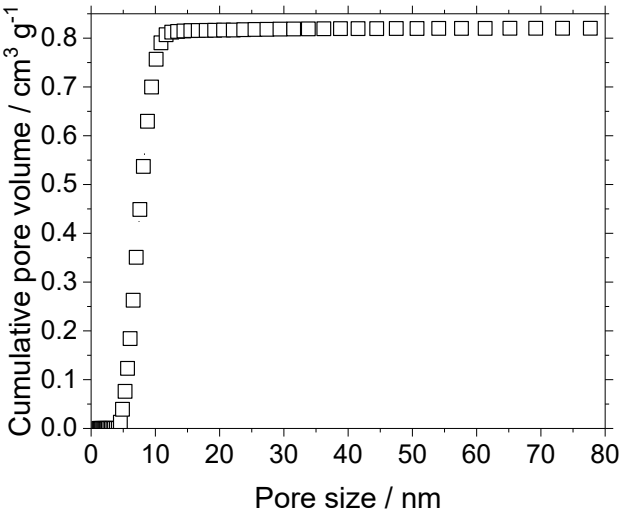

Figure S9. Resulting cumulative pore volume obtained from NLDFT-calculations (adsorption branch) for silica fraction 450 - 630 µm, untreated.

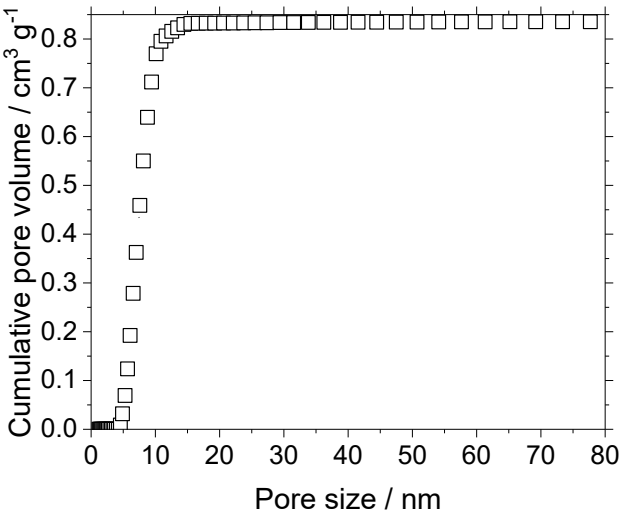

Figure S10. Resulting cumulative pore volume obtained from NLDFT-calculations (adsorption branch) for silica fraction 630 - 800 µm, untreated.

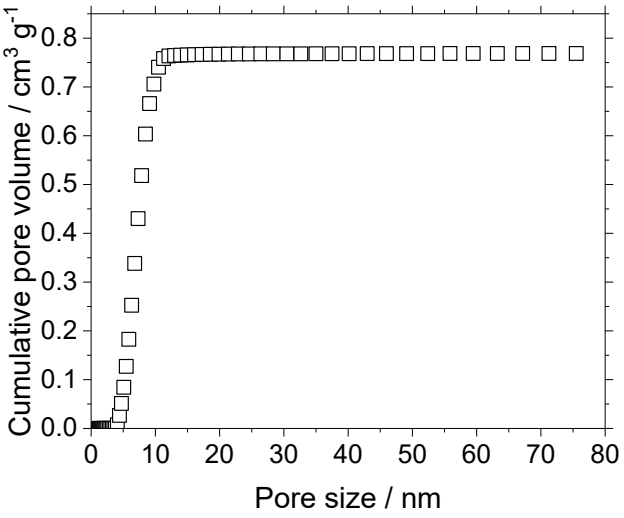

Figure S11. Resulting cumulative pore volume obtained from NLDFT-calculations (adsorption branch) for silica fraction 800 – 1000 µm, untreated.

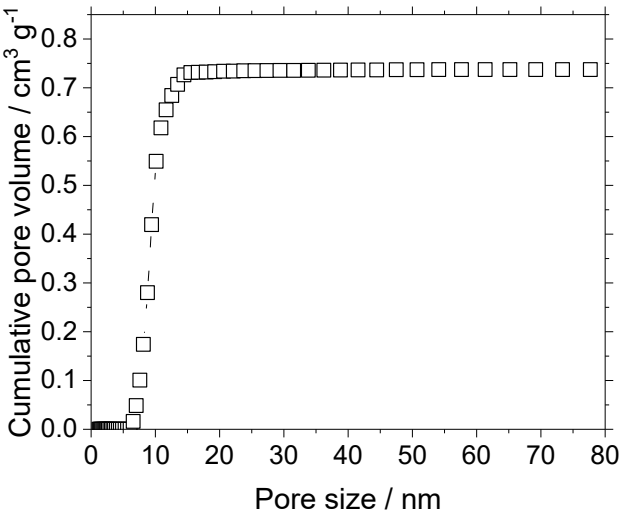

Figure S12. Resulting cumulative pore volume obtained from NLDFT-calculations (adsorption branch) for silica fraction 63 – 200 µm, hydrothermally treated at 120 °C for 9 h.

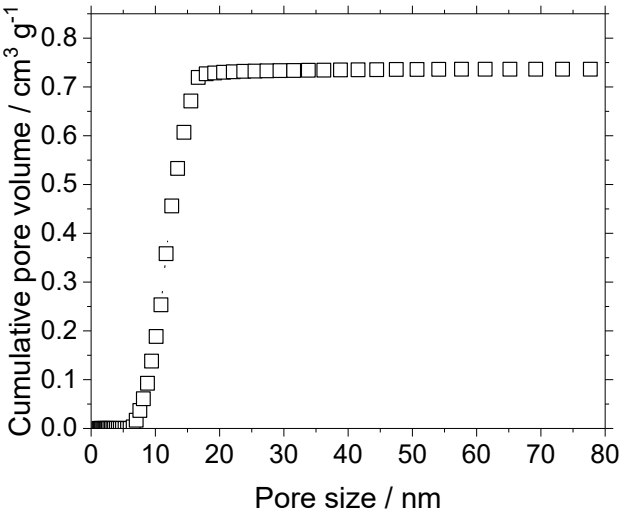

Figure S13. Resulting cumulative pore volume obtained from NLDFT-calculations (adsorption branch) for silica fraction 63 – 200 µm, hydrothermally treated at 120 °C for 16 h.

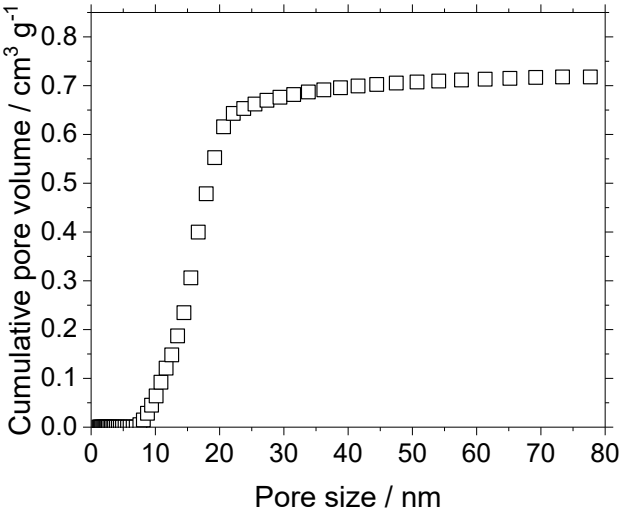

Figure S14. Resulting cumulative pore volume obtained from NLDFT-calculations (adsorption branch) for silica fraction 63 – 200 µm, hydrothermally treated at 120 °C for 24 h.

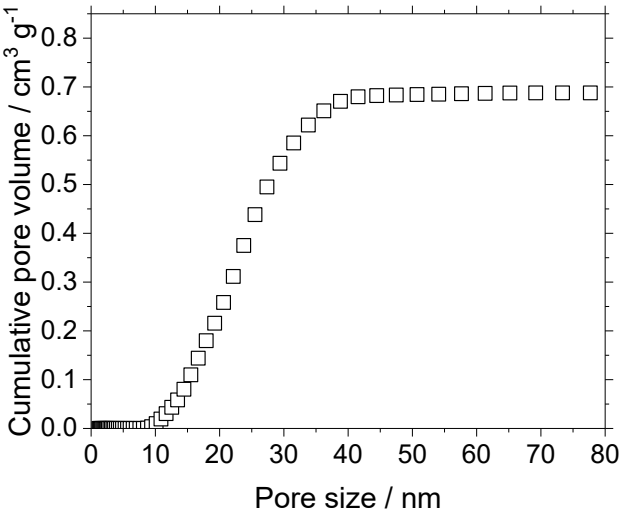

Figure S15. Resulting cumulative pore volume obtained from NLDFT-calculations (adsorption branch) for silica fraction 63 – 200 µm, hydrothermally treated at 120 °C for 100 h.

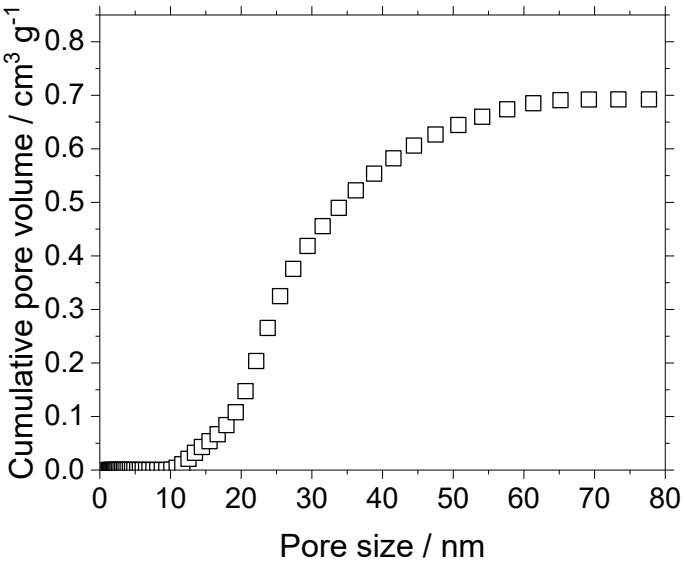

Figure S16. Resulting cumulative pore volume obtained from NLDFT-calculations (adsorption branch) for silica fraction 63 – 200 µm, hydrothermally treated at 120 °C for 200 h.

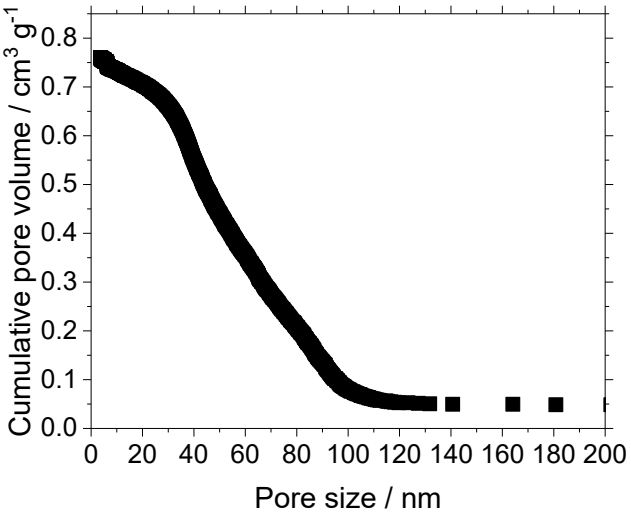

Figure S17. Resulting cumulative pore volume obtained from MPI measurement for silica fraction 63 – 200 µm, hydrothermally treated at 180 °C for 24 h.

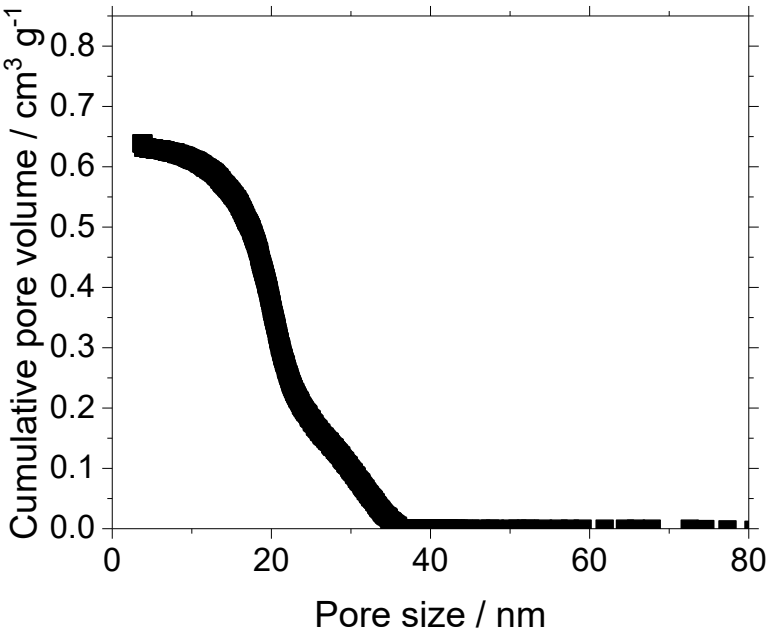

Figure S18. Resulting cumulative pore volume obtained from MPI measurement for silica fraction 63 – 200 µm, hydrothermally treated at 150 °C for 24 h.

CO_2 TPD measurements

We used pure ammonia and pure CO2. We know that diluted streams are preferably used but the TPD device in its configuration at that time could not. To account for the non-diluted streams we had a long flushing period of inert gas afterwards.

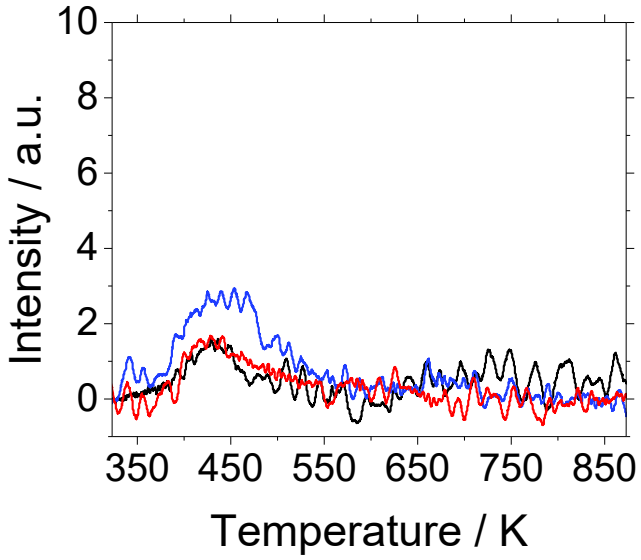

Figure S19. CO_2-TPD measurement of untreated silica (black), hydrothermally treated at 120 °C for 24 h (blue) and hydrothermally treated at 120 °C for 100 h (red). All samples were calcined at 600 °C before measuring as well as before reaction.

The precise values of the concentrations are 1.55 µmol g^{-1} for the untreated material, 2.07 µmol g^{-1} for the sample treated at 24 h and 1.10 µmol g^{-1}. As the signal-to-noise ratio is high and the signal intensities are small we decided to round the values accordingly. Hence, the concentration of the untreated sample and the sample treated for 24 h end up at the same concentration of ≤ 2 µmol g^{-1}.

Benson group contribution model

Table S1: Group contributions for 2-propyl-2-heptenal and 3-hydroxy-2-propylheptenal using the Benson group contribution model in Aspen Plus V10.

2-propyl-2-heptenal		3-hydroxy-2-propylheptenal	
Group number	number of occurences	Group number	number of occurences
100	2	100	2
101	3	101	5
105	1	172	1
119	2	189	1
167	1	199	1
191	1	210	1

Reaction results

exemplary GC measurment

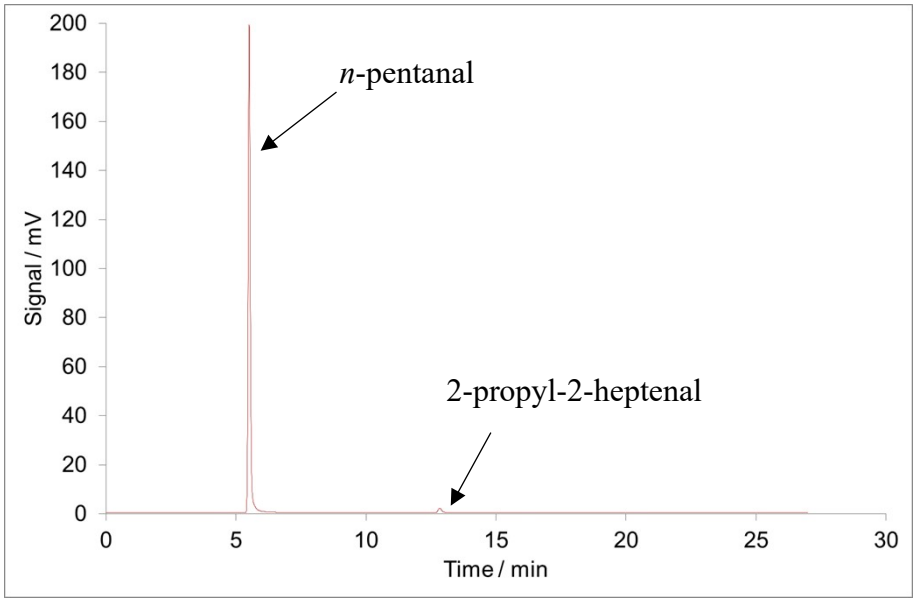

Figure S20. GC chromatogram of the gas-phase aldol condensation of *n*-pentanal.

Start-up behavior

We then investigated the initial phase of the experiment in more detail. As shown in Figure S21, a very different behavior was observed in the on-line GC regarding *n*-pentanal amount for an experiment without support, with a macro-porous support and with a meso-porous support. Before every experiment, the reactor was filled with inert helium (see experimental section). Using no support, only the first injection after 0.03 h showed a smaller amount of *n*-pentanal due to the dilution with helium in the reactor. After the first injection, the signal stabilized and did not change significantly over the next 50 min. This is a clear indication that the *n*-pentanal flow reached steady state during the first injection. A similar behavior was found for the macro-porous support. However, when using the mesoporous support, an adsober-like behavior was observed in the first 0.2 h TOS where no substrate was detected in the product stream. After 0.25 h, the signal increases rapidly to the initial value.

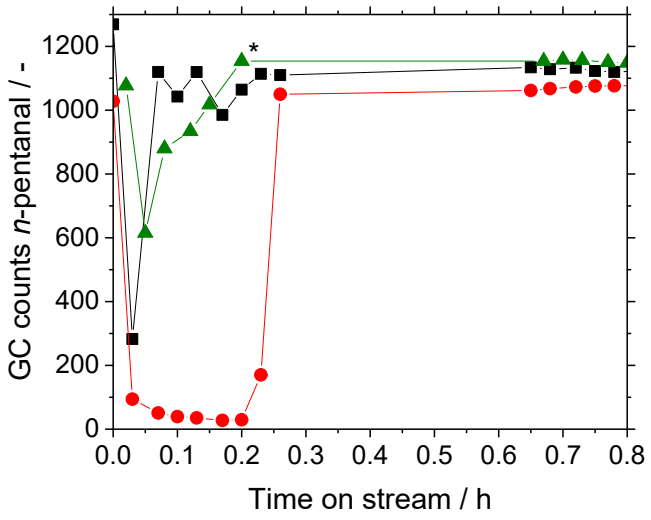

Figure S21. GC counts of substrate *n*-pentanal after directing feed gas to empty reactor (O), reactor filled with 2 g silica particles (63 – 200 µm fraction) with a median pore size of 7 nm (ᔓ) and, 2 g silica particles (63 – 200 µm fraction) with a median pore size of 54 nm (□). * Data point

interpolated. Reaction conditions: T = 373 K, $p_{n\text{-pentanal}}$ = 10 kPa, $\dot{m}_{n-\text{pentanal}}$ = 0.02 g min^{-1}, $\dot{V}_{\text{helium}}$ = 50 ml$_N$ min^{-1}.

Calculated values for r_0 as a function of temperature

Table S2: Calculated reaction rates r_0 for different temperatures.

T / °C	100	120	140	164	188
r_0 / 10^{-3} mmol h^{-1} m^{-2}	0.21	0.42	0.82	1.29	1.66

Temperature dependency of k_d

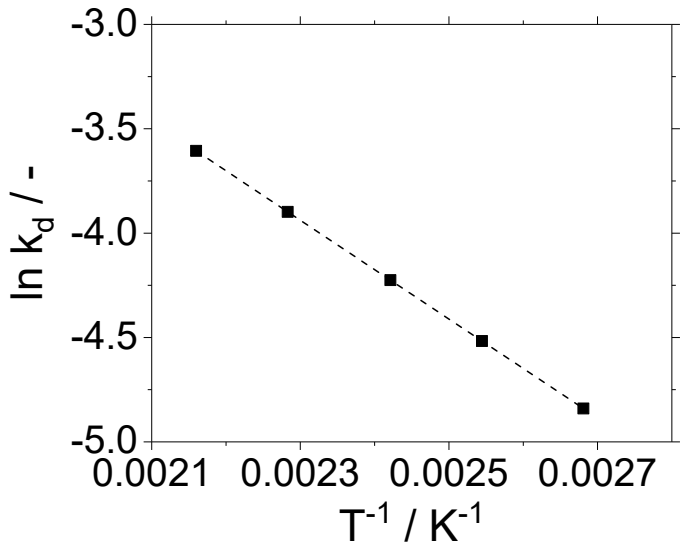

Figure S22. Temperature dependency of deactivation rate constant k_d in the temperature range of 100 to 188 °C.

Activity graph for different substrate partial pressures

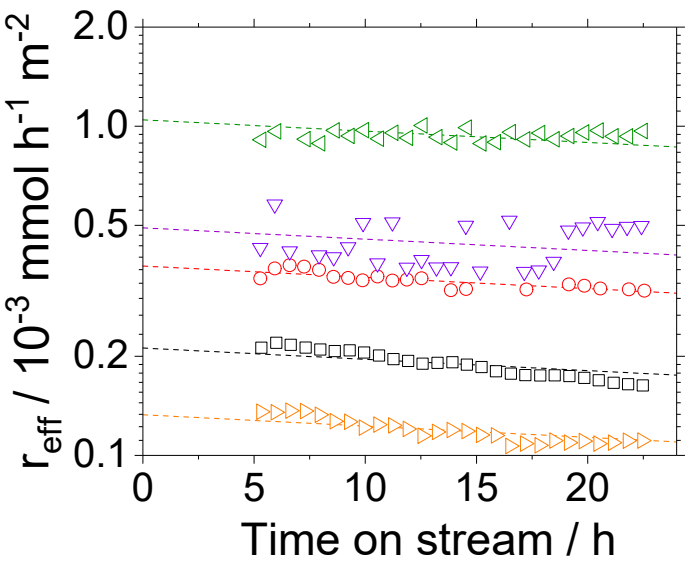

Figure S23. Measured effective reaction rates r_{eff} over time for different n-pentanal partial pressures: 5 kPa (◆), 10 kPa (●), 20 kPa (ᔓ), 30 kPa (♦), 50 kPa (❖). Reaction conditions: m_{Silica} = 2.00 g, T = 100 °C, $\dot{m}_{pentanal}$ = 0.02 g min^{-1}, $\dot{V}_{helium}$ = 50 ml_N min^{-1}.

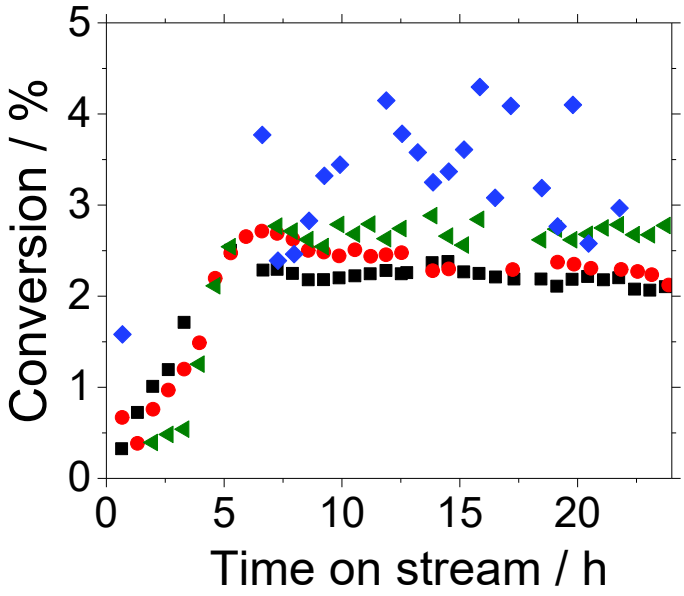

Figure S24. Conversion of *n*-pentanal for different partial pressures: 10 kPa (●), 20 kPa (ᔓ), 50 kPa (♦), 70 kPa (◆). Reaction conditions: m_{Silica} = 2.00 g, T = 100 °C, $\dot{m}_{pentanal}$ = 0.02 g min^{-1}, $\dot{V}_{helium}$ = 50 ml_N min^{-1}.

Kelvin-equation calculations with σ, Q after Bird/Brock/Miller VDI heat atlas, D1, page 170 [1]:

$$p = p_s * \exp\left(-\frac{2\sigma M}{RT\delta_l} * \frac{1}{r_{pore}}\right) \quad \text{S1}$$

$$\frac{\sigma}{mN/m} = \left(\frac{p_c}{bar}\right)^{\frac{2}{3}}\left(\frac{T_c}{K}\right)^{\frac{1}{3}} Q(1 - T_r)^{11/9} \quad \text{S2}$$

$$Q = 0{,}1196\left(1 + \frac{\frac{T_{NBP}}{T_c}\ln\frac{p_c}{1.01325\ bar}}{1 - \frac{T_{NBP}}{T_c}}\right) \quad \text{S3}$$

with M = 86.13 g mol^{-1}, T_{NBP} = 375.8 K, T_c = 554 K, p_c = 35.5 bar, δ_l = 747.3 kg m^{-3},

Activity graph for different particle sizes

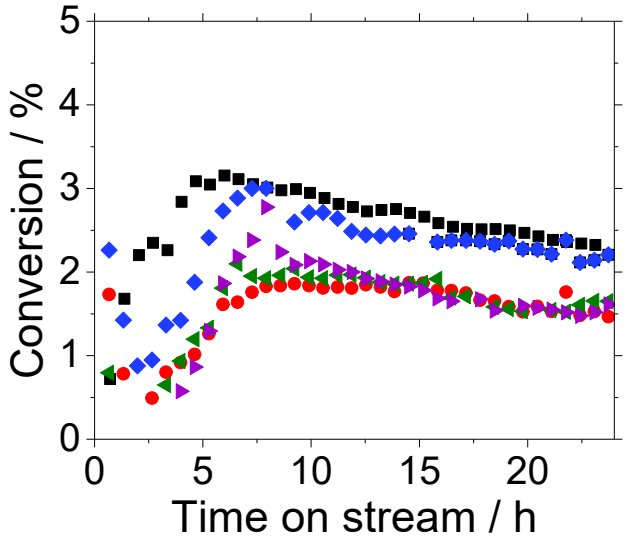

Figure S25. Conversion of n-pentana for different particle size fractions: Reaction conditions: 63 – 200 µm (●), 200 – 450 µm (ᔓ), 450 – 630 µm (♦), 630 – 800 µm (◆), 800 – 1000 µm (◆). Reaction conditions: m_{Silica} = 2.00 g, T = 100 °C, $p_{pentnal}$ = 0.01 bar, $\dot{m}_{pentanal}$ = 0.02 g min^{-1}, $\dot{V}_{helium}$ = 50 ml$_N$ min^{-1}.

Activity graphs for different pore sizes

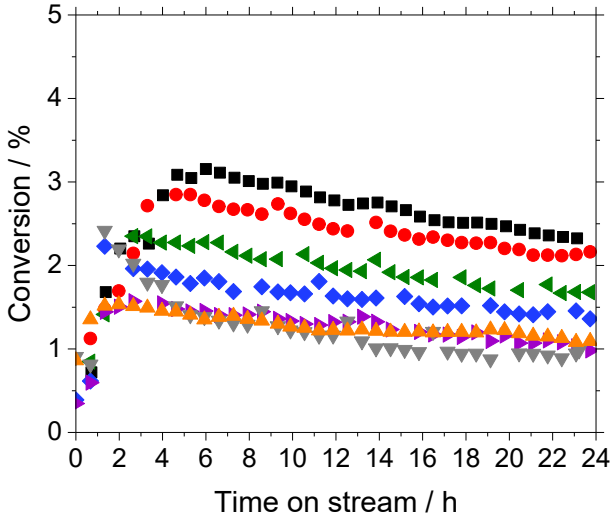

Figure S26. Conversion of *n*-pentnal for silica particle fractions with different median pore sizes: d_{50} = 7 nm (●), d_{50} = 9 nm (ᔓ), d_{50} = 12 nm (♦), d_{50} = 16 nm (◴), d_{50} = 23 nm (◆), d_{50} = 26 nm (❑), d_{50} = 54 nm (□). Reaction conditions: m_{Silica} = 2.00 g, T = 100 °C, $p_{pentnal}$ = 0.01 bar, $\dot{m}_{pentanal}$ = 0.02 g min^{-1}, $\dot{V}_{helium}$ = 50 ml_N min^{-1}.

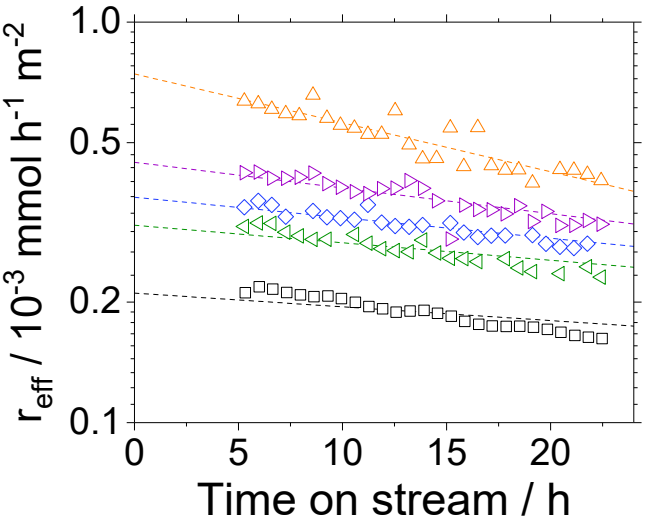

Figure S27. Effective reaction rate (d_{50} = 7 nm (⭘), d_{50} = 12 nm (❖), d_{50} = 16 nm (❋), d_{50} = 23 nm (⬥), d_{50} = 54 nm (❒)) for silica particles (63 – 200 µm fraction) with different median pore sizes. Reaction conditions: TOS = 24 h, m_{Silica} = 2.00 g, T = 373 K, $p_{n\text{-pentanal}}$ = 10 kPa, $\dot{m}_{n-\text{pentanal}}$ = 0.02 g min^{-1}, $\dot{V}_{\text{helium}}$ = 50 ml$_N$ min^{-1}.

TGA measurments

A calcination temperature of 873 K was set as benchmark for SILP hydroformylation in former studies and was kept here to use similar treated supports. Literature suggests that strong acidic sites can give a peak up to 1000 K (Lónyi and Valyon, DOI: 10.1016/s1387-1811(01)00389-4). Therefore we set the temperature of the TPD measurements to 1073 K.

Table S3: Thermogravimetric analysis results of silica samples used for different times on stream (TOS). Reaction conditions: $d_{particle}$ = 63 – 200 µm, d_{50} = 7 nm, T = 100 °C, $p_{n\text{-pentanal}}$ = 0.1 bar.

TOS[1]	$\Delta m_{n\text{-pentanal}}$[2]	Δm_{aldol}[2]	$\Delta m_{\text{higher hydrocarbons}}$[2]	$\alpha_{n\text{-pentanal}}$[2]	α_{aldol}[2]	$\alpha_{\text{higher hydrocarbons}}$[2]
h	mg	mg	mg	%	%	%
1	2.18	2.24	1.22	6.93	7.13	3.87
12	1.99	4.42	1.46	6.97	15.5	5.11
24	3.63	5.08	1.88	11.5	16.1	5.93
60	1.45	5.65	1.90	5.76	22.5	7.54
100	1.80	6.62	1.65	6.85	25.2	6.29
130	1.83	7.34	1.67	7.49	30.0	6.81
24	0.17	1.10	0.35	0.57	3.69	1.18
60	0.15	0.97	0.33	0.49	3.29	1.13
100	0.03	1.14	0.44	0.01	3.78	1.46

[1] reaction conditions, [2] obtained from thermogravimetic analysis

Table S4: Thermogravimetric analysis results of silica samples used at different *n*-pentanal partial pressures ($p_{n\text{-pentanal}}$). Reaction conditions: $d_{particle}$ = 63 – 200 µm, d_{50} = 7 nm, T = 100 °C, TOS = 24 h.

$p_{n\text{-pentanal}}$[1]	$\Delta m_{n\text{-pentanal}}$[2]	Δm_{aldol}[2]	$\Delta m_{higher\ hydrocarbons}$[2]	$\alpha_{n\text{-pentanal}}$[2]	α_{aldol}[2]	$\alpha_{higher\ hydrocarbons}$[2]
bar	mg	mg	mg	%	%	%
0.05	1.96	5.19	1.48	6.52	17.3	4.93
0.1	3.63	5.08	1.88	11.5	16.1	5.93
0.2	2.06	7.00	1.69	7.49	25.5	6.13
0.3	11.64	6.28	1.41	56.3	30.4	6.81
0.5	9.68	6.26	3.11	50.5	32.6	16.2
0.7	15.72	2.76	0.93	76.6	13.4	4.54

[1] reaction conditions, [2] obtained from thermogravimetic analysis

Table S5: Thermogravimetric analysis results of silica samples used at different reaction temperatures (T). Reaction conditions: $d_{particle}$ = 63 – 200 µm, d_{50} = 7 nm, $p_{n\text{-}pentanal}$ = 0.1 bar, TOS = 24 h.

T[1]	$\Delta m_{n\text{-}pentanal}$[2]	Δm_{aldol}[2]	$\Delta m_{higher\ hydrocarbons}$[2]	$\alpha_{n\text{-}pentanal}$[2]	α_{aldol}[2]	$\alpha_{higher\ hydrocarbons}$[2]
°C	mg	mg	mg	%	%	%
100	3.63	5.08	1.88	11.5	16.1	5.93
120	2.31	4.56	1.51	7.44	14.7	4.88
140	1.15	3.59	1.39	3.95	12.3	4.78
164	1.57	2.98	1.50	4.77	9.06	4.56
188	1.05	3.11	1.39	3.73	11.1	4.95

[1] reaction conditions, [2] obtained from thermogravimetic analysis

Table S6: Thermogravimetric analysis results of silica samples with different particle size fractions. Reaction conditions: d_{50} = 7 nm, T = 100 °C, $p_{n\text{-}pentanal}$ = 0.1 bar, TOS = 24 h.

$d_{particle}$[1]	$\Delta m_{n\text{-}pentanal}$[2]	Δm_{aldol}[2]	$\Delta m_{higher\ hydrocarbons}$[2]	$\alpha_{n\text{-}pentanal}$[2]	α_{aldol}[2]	$\alpha_{higher\ hydrocarbons}$[2]
µm	mg	mg	mg	%	%	%
63–200	3.63	5.08	1.88	11.5	16.1	5.93
200–450	2.93	5.55	1.83	10.0	19.0	6.27
450–630	2.53	5.47	1.84	8.31	20.3	6.37
630–800	2.05	5.41	1.58	7.72	20.4	5.97
800–1000	2.49	6.10	1.91	8.86	21.7	6.79

[1] reaction conditions, [2] obtained from thermogravimetic analysis

Table S7: Thermogravimetric analysis results of silica samples with different median pore size d_{50}. Reaction conditions: $d_{particle}$ = 63 – 200 µm, T = 100 °C, $p_{n\text{-}pentanal}$ = 0.1 bar, TOS = 24 h.

d_{50}[1]	$\Delta m_{n\text{-}pentanal}$[2]	Δm_{aldol}[2]	$\Delta m_{higher\ hydrocarbons}$[2]	$\alpha_{n\text{-}pentanal}$[2]	α_{aldol}[2]	$\alpha_{higher\ hydrocarbons}$[2]
nm	mg	mg	mg	%	%	%
7	3.63	5.08	1.88	11.5	16.1	5.93
9	2.44	4.02	1.33	7.63	12.6	4.15
12	1.52	2.89	0.96	5.53	10.6	3.49
16	1.14	2.49	0.74	4.12	9.01	2.69
23	0.44	1.98	0.65	1.42	6.39	2.09
54	0.17	1.10	0.35	0.57	3.69	1.18

[1] reaction conditions, [2] obtained from thermogravimetic analysis

Calculation of product streams

The total product stream was calculated using the known helium throughput and the composition of the product gas.

$$\dot{n}_{ges,out} = \frac{\dot{n}_{He,in}}{x_{He,out}}$$

Using the calibrated composition of *n*-pentanal in the product stream $x_{n\text{-}pentanal,out}$ the outlet flow was calculated with

$$\dot{n}_{n\text{ - }pentanal,out} = \dot{n}_{ges,out} * x_{n\text{ - }pentanal,out}$$

The calibration of 2-propyl-2-heptenal was calculated from the *n*-pentanal calibration using the effective carbon number according to Scalnon and Willis (DOI: 10.1093/chromsci/23.8.333).

References

1. *VDI-Wärmeatlas: Mit 320 Tabellen. VDI-Buch.*, 11 edn. Springer Vieweg: Berlin, 2013.